ACR July 1939

[redacted]

NATIONAL ADVISORY COMMITTEE FOR AERONAUTICS

WARTIME REPORT

ORIGINALLY ISSUED
July 1939 as
Advance Confidential Report

AERODYNAMIC CHARACTERISTICS OF A 4-ENGINE MONOPLANE SHOWING COMPARISON OF AIR-COOLED AND LIQUID-COOLED ENGINE INSTALLATIONS

By Abe Silverstein and Herbert A. Wilson, Jr.

Langley Memorial Aeronautical Laboratory
Langley Field, Va.

NACA

WASHINGTON

NACA WARTIME REPORTS are reprints of papers originally issued to provide rapid distribution of advance research results to an authorized group requiring them for the war effort. They were previously held under a security status but are now unclassified. Some of these reports were not technically edited. All have been reproduced without change in order to expedite general distribution.

L - 471

AERODYNAMIC CHARACTERISTICS OF A 4-ENGINE MONOPLANE SHOWING COMPARISON OF AIR-COOLED AND LIQUID-COOLED ENGINE INSTALLATIONS

By Abe Silverstein and Herbert A. Wilson, Jr.

SUMMARY

An investigation has been conducted in the N.A.C.A. full-scale wind tunnel of a 1/4-scale model of a large 4-engine monoplane to determine the over-all aerodynamic efficiency of comparable liquid-cooled and air-cooled engine installations.

The results show that the nacelles for liquid-cooled engines increased the high-speed drag of the model 7.9 percent, the oil coolers 3.9 percent, and the underslung Prestone radiators 13.5 percent, making the total drag increase of the installation 25.3 percent.

The nacelles for the air-cooled engines increased the high-speed drag of the model 16.8 percent, the oil coolers 3.9 percent, and the cooling air 16.8 percent, making the total drag increase of the installation 37.5 percent. A slightly higher propulsive efficiency for the air-cooled installation partially offset its higher drag.

The oil coolers in the leading edge of the wing considerably decreased the maximum lift coefficient.

INTRODUCTION

An investigation has been conducted in the N.A.C.A. full-scale wind tunnel to determine the aerodynamic characteristics of a 1/4-scale model of a 4-engine monoplane when equipped with comparable air-cooled and liquid-cooled engine installations. The air-cooled engine installation consisted of nacelles equipped with N.A.C.A. cowlings and oil coolers located in the leading edge of the wing. The liquid-cooled arrangement consisted of nacelles with underslung Prestone radiators and oil coolers in the leading edge of the wing. In each case the maximum nacelle diameters and fairing of the nacelles into the wing were identical.

The investigation included measurements of the lift, the drag, and the pitching moment coefficients of the model, and of the propulsive efficiency of the engine-propeller installations for the following conditions.

A. Bare wing model without nacelles, radiators, or oil coolers (fig. 1).

B. Air-cooled engine installations (fig. 2).

(1) With N.A.C.A. cowlings having large exit slots, and oil coolers in the leading edge of the wing.

(2) With oil coolers closed.

(3) With oil coolers closed and without air flow through the cowling.

(4) With oil coolers closed and with exit slots of cowlings refaired and decreased in size.

C. Liquid-cooled engine installations (fig. 3).

(1) With nacelles, underslung Prestone radiators, and oil coolers in leading edge of the wing.

(2) With Prestone radiators removed.

(3) With Prestone radiators removed and oil coolers closed.

The 1/4-scale model is the same one used in a previous investigation of enclosed-engine arrangements reported in reference 1.

SYMBOLS

α_T, angle of attack of the fuselage reference axis relative to the wind axis, deg.

q, dynamic pressure, lb. per sq. ft.

S, wing area, sq. ft.

$\bar{c}$, mean chord of the wing, area/span, ft.

V, air speed, f.p.s.

L, lift, or force normal to the relative wind, lb.

D, drag, or force parallel to the relative wind, lb.

D_c, power-off drag of combination, lb.

M, pitching moment, lb.-ft.

$C_L = L/qS$

$C_D = D/qS$ (Subscript w refers to power-off drag of the model with <u>bare wing</u>; c, to power-off drag of the model with <u>engine-nacelle installation</u>.)

$C_m = M/qS\bar{c}$

R, resultant drag force of a propeller-body combination, lb.

T, thrust of propellers operating in front of a body (tension in propeller shafts), lb.

ΔD, increase in drag of the body behind the propellers due to the action of the propellers.

$T - \Delta D$, effective thrust of the propeller-body combination.

T_o, index thrust.

P, power input per propeller.

$P_{tot.}$, total power input to propellers.

$$C_T = \frac{T - \Delta D}{\rho n^2 D^4}$$

$$C_P = \frac{P}{\rho n^3 D^5}$$

$$\eta = \frac{(T - \Delta D)\,V}{P} = \text{propulsive efficiency.}$$

$$\eta_t = \eta\left(\frac{C_{D_w}}{C_{D_c}}\right) = \text{over-all efficiency.}$$

$$T_{c_o}' = \frac{P_{tot.}\ \eta_o}{\frac{1}{2}\ \rho\ V^3\ S} = \text{index thrust coefficient.}$$

$\eta_o = \eta$ at $C_L = 0.25$.

n, propeller revolution speed, r.p.s.

D, propeller diameter, ft.

β, propeller blade angle at 0.75 R, deg.

δ_f, flap deflection from closed position, deg.

a, slope of lift curve, $dC_L/d\alpha$, deg.

MODEL AND TEST EQUIPMENT

The tests were conducted in the N.A.C.A. full-scale wind tunnel, a description of which is given in reference 2.

The model was a metal-covered, midwing monoplane with a span of 37.25 feet. The wing sections were symmetrical and tapered in thickness from 0.18c at the root to 0.10c at the tip. The wing had a plan form tapered 4:1, with a root chord of 7.28 feet and an area of 172 square feet. Split trailing-edge flaps with an average chord of 0.15c extended over the middle 60 percent of the span with the exception of a short gap at the fuselage. The angle of wing setting to the fuselage reference line was 4.6°. A line diagram of the model with dimensions of the various nacelle-propeller arrangements tested is shown in figure 4.

Four 3-blade aluminum alloy model propellers were used throughout the tests. Blade dimensions and sections for the propellers are given in figure 5. Each propeller was driven by a 25-horsepower squirrel-cage induction motor, the speed of which was regulated by varying the frequency. The propeller speed was measured with a Weston electrical tachometer. Propeller torques were determined from an electrical calibration of the motors.

Perforated metal plates were used to simulate the radiators for the liquid-cooled engine installation, and the engines for the air-cooled engine installations. The plates simulating the radiators were proportioned to have the same resistance as a standard Army Air Corps radiator of 9-inch depth. Holes were spaced in the 13-inch-diameter plate used to simulate the air-cooled engine so as to obtain a conductivity, k, of 0.124 (see reference 3), which approximates that of a twin-row radial engine. The cowling was tested with the originally designed exit slot 1-3/16 inches and the reduced slot of 3/4 inch width (fig. 4) which have been designated as large exit slot and refaired exit slot, respectively. A pressure drop across the conductivity plates of 1.29 q was measured with the large exit slots and 0.63 q with the refaired slots.

TESTS

With the propellers removed from the model, measurements of forces and pitching moments were made for all the test arrangements over an angle-of-attack range from zero lift through the stall at an air speed of about 60 miles per hour. Scale effect on the drag at low lift coefficients was also measured over a range of air speeds from 30 to 120 miles per hour.

With the propellers operating, propulsive characteristics of the nacelle-propeller arrangements were determined for an angle of attack corresponding to high-speed flight. In addition to the usual aerodynamic forces and pitching moment, the measurements included the power input to the propellers and the propeller speed. The procedure followed in the propeller tests was to hold the torque constant and increase the tunnel air speed in steps from 30 miles per hour to 100 miles per hour, after which the propeller speed was reduced until zero thrust was reached. The effect of the propeller operation upon the lift and the pitching moment was determined at a tunnel speed of approximately 50 miles per hour for several thrust conditions.

POWER-OFF CHARACTERISTICS

Aerodynamic characteristics of the model with the propellers removed are shown in figures 6 to 13. The data shown in figures 6 to 10 were obtained at a test speed of about 60 miles per hour corresponding to a Reynolds Number of approximately 2,500,000, based on the average wing chord of 4.62 feet. The coefficients are based on a wing area of

172 square feet and are corrected for wind-tunnel effects. Pitching-moment coefficients are computed about the assumed center-of-gravity position shown in figure 5. A comparison of the more important characteristics such as L/D_{max}, $C_{L_{max}}$, C_D at $C_L = 0.25$, etc., is given in table I.

Drag.- The scale effect on the drag coefficients of the various model arrangements at $C_L = 0.25$ (assumed high-speed lift coefficient) is shown in figures 11 and 12. The drag coefficients obtained at 100 miles per hour are used for the comparison of the arrangements in table I. The drag increments due to the nacelles, radiators, cowlings, etc., are shown in figure 13.

Based on the bare-wing model drag, the tests show that the liquid-cooled engine nacelles increase the drag coefficient of the model by 0.0014, or 7.9 percent; the oil coolers increase the drag by 0.0007, or 3.9 percent; and the Prestone radiators increase the drag by 0.0024, or 13.5 percent. The total increase in drag coefficient due to the liquid-cooled engine installation is 0.0045, or 25.3 percent.

The increase in drag coefficient due to the air-cooled engine nacelles and cowlings with no cooling air is 0.0030 or 16.8 percent of the bare-wing model drag. With the cooling air flowing through the large exit slot of the cowlings the drag coefficient of the nacelles is increased to 0.0060 or 33.7 percent. Including the 3.9-percent increase due to the oil coolers, the total drag of the air-cooled engine installations with large exit slots is 0.0067 or 37.6 percent of the bare-wing model drag. By reducing the exit slot gap to 3/4 inch, eliminating the sharp corner of the nacelle at the cowling exit slot, and providing a smooth contour, the drag of the air-cooled installation was reduced to 0.0054 or 30.4 percent of the bare-wing model drag.

Maximum lift.- Values of maximum lift for the various arrangements are shown in table I. There is little variation in the maximum lift coefficients for the air-cooled engine arrangements; however, they show a small increase over the values obtained for the bare-wing case. This increase may possibly be attributed to an increase in the effective area of the wing due to the nacelles.

Of particular interest is the comparatively low value of the maximum lift coefficient for the liquid-cooled engine arrangement with oil coolers open. Unfortunately, the maximum lift coefficient was not determined for the air-cooled engine arrangement with oil coolers open; however, a study of tuft surveys made on the liquid-cooled engine arrangement (reference 1) indicates that the oil coolers seriously disturb the air flow over the wing at large angles of attack, thereby inducing an earlier separation and lower maximum lift coefficient.

PROPULSIVE AND OVER-ALL EFFICIENCIES

Engine-propeller combinations should be compared by means of an over-all efficiency including both drag and propulsive efficiency. The over-all efficiency is defined as the ratio of the power required for the bare-wing model at a given level flight speed to the power input actually required at this speed for the model with the engine-propeller installation.

The over-all efficiency of the bare-wing model is therefore 100 percent and, for an engine-propeller combination, is given by

$$\eta_t = \eta \left(\frac{C_{D_W}}{C_{D_c}}\right)$$

Values of over-all efficiency given in table I are based on a lift coefficient, $C_L = 0.25$, and a blade angle, $\beta = 23\frac{1}{2}^\circ$ at 0.75 R, which are assumed high-speed conditions.

The effective thrust of a propeller-body combination may be computed from wind-tunnel data by means of the relation

$$R = D_c + \Delta D - T$$

from which,

$$T - \Delta D = D_c - R$$

For tests without a lifting surface behind the propeller, $T - \Delta D$ may be obtained from measurements of D_c and R made at the same angle of attack and dynamic pressure.

When the flow over a lifting surface is influenced by the propeller, there are changes in the lift as well as the drag that should be credited to or charged against the propeller. The change in lift has been allowed for in these results by making measurements of D_c and R at the same lift coefficient instead of at the same angle of attack.

Propulsive characteristics at $C_L = 0.25$ are shown in figures 14 and 15 for the air-cooled engine installations and in figure 16 for the liquid-cooled engine installations. The propulsive efficiencies for the air-cooled installations at $C_L = 0.70$ are almost identical with those at $C_L = 0.25$. The propulsive efficiencies for the air-cooled installations with large exit slots (fig. 14) increase with blade angle up to $\beta = 33\frac{1}{2}°$, reaching a maximum efficiency of 84.5 percent. The liquid-cooled installation reaches a maximum value of 81 percent at $\beta = 23\frac{1}{2}°$ and decreases slightly for $\beta = 28\frac{1}{2}°$. The higher efficiency of the air-cooled installations is attributed to an improvement in flow over the air-cooled cowlings due to the propeller slipstream. The high propulsive efficiency of propellers operating ahead of bodies over which the flow is disturbed has been noted in previous investigations. This latter supposition is borne out by the data shown in figure 15 for the air-cooled installations with the refaired exit slot. For this condition, the exit slot was refaired so that the air flow was more nearly tangential to nacelle contour than for the original sharp-edge exit slot. The propulsive efficiency for this case closely corresponds to that for the liquid-cooled installation. The over-all efficiencies, η_t, given in table I, show that the over-all efficiency of the liquid-cooled installation is about $64\frac{1}{2}$ percent, whereas that for the air-cooled installation with large exit slot is only 60 percent.

POWER-ON CHARACTERISTICS

In order to describe the conditions of propeller operation and avoid the complexities introduced by variations in propeller blade angle and V/nD, use is made of an index thrust coefficient, which is independent of these variables, and takes the form

$$T_{c_o}' = \frac{T_o}{qS} = \frac{P\eta_o}{qSV}$$

in which η_o is the propulsive efficiency at $C_L = 0.25$ for the conditions of V/nD and blade angle at which the tests were made. The variations of the lift curves of the air-cooled arrangements with T_{c_o}' are shown in figures 17 and 18, and the variations of maximum lift coefficient and lift curve slope are shown in figure 19. The effects of power on lift are more pronounced for the case of flaps up than for flaps down, and the variation for index thrust coefficients greater than 0.1 is almost linear. For index thrust coefficients less than 0.1, the increase in lift with flaps down with T_{c_o}' is quite large. It will be noted that the maximum lift coefficients, flaps up and flaps down, converge for high values of index thrust coefficient.

A large change of the pitching moment with application of power is shown by figures 20, 21, and 22, for the air- and liquid-cooled engine installations with flaps up, and for the air-cooled engine installation with flaps down. Figures 20 and 21 show that for both installations with flaps up there is a change in balance with increasing power, but no large change in stability. For the air-cooled engine installation with flaps down, however, there is a smaller change in balance accompanied by a very large change in static stability, the model becoming quite unstable at large values of thrust.

HIGH-SPEED PERFORMANCE COMPARISON

In order to compare the engine installations directly on a basis of the performance of the full-scale airplane, a high-speed determination has been made for all of the model arrangements in figures 23 and 24. The calculations are based on sea-level air density, a gross weight of 70,570 pounds, a wing area of 2,750 square feet, a propeller diameter of 13 feet, constant-speed propeller operation at 1,300 r.p.m., and a total engine output of 4,000 horsepower. Curves of lift against drag are taken from data at 100 miles per hour tunnel speed.

Values of the high speed for each of the model arrangements are shown in table I. The high speed for the complete air-cooled engine installation is 192 miles per hour as compared with 195 miles per hour for the complete liquid-cooled installation. An interesting comparison is found in items 6 and 8 of table I, from which it is seen that changing from a liquid-cooled nacelle exclusive of cooling to an air-cooled nacelle with no cooling decreases the maximum speed from 207 miles per hour to 200.5 miles per hour. This difference is due to the fact that the drag increment for the air-cooled nacelles is more than double that for the liquid-cooled nacelles.

CONCLUDING REMARKS

The aerodynamic characteristics of the model tested with the liquid-cooled engine installation are somewhat superior to those of the air-cooled engine installation with the original exit slot. The lower propulsive efficiency of the liquid-cooled installation is more than compensated for by the lower drag. Changing the nacelle from the streamline shape of the liquid-cooled installation to the blunt shape of the air-cooled installation about doubles the nacelle drag. Comparison of the drag results for the air-cooled engine installation with the large exit slot and with the refaired exit slot emphasizes the necessity for providing an N.A.C.A. cowling with a smooth exit slot and of correctly adjusting the quantity of flow through the cowling.

The refaired exit slot arrangement represents a design providing sufficient cooling for climbing flight and excessive cooling drag for the high-speed condition. The use of an exit slot large enough to cool the engine in the high-speed condition, in combination with a means for increasing the exit slot area during climbing flight, would reduce the cooling drag to a negligible quantity. A corresponding reduction in the cooling drag of the liquid-cooled engine installation could be accomplished by the use of wing-duct radiators described in reference 4. General comparisons of the merits of liquid-cooled and air-cooled engine installations are not feasible from the limited data presented in this report.

Langley Memorial Aeronautical Laboratory,
National Advisory Committee for Aeronautics,
Langley Field, Va., December 5, 1938.

REFERENCES

1. Silverstein, Abe, and Wilson, Herbert A., Jr.: Aerodynamic Characteristics of a 4-Engine Monoplane Showing Effects of Enclosing the Engines in the Wing and Comparisons of Tractor- and Pusher-Propeller Arrangements. NACA ACR, April 1938.

2. DeFrance, Smith J.: The N.A.C.A. Full-Scale Wind Tunnel. NACA Rep. No. 459, 1933.

3. Theodorsen, Theodore, Brevoort, M. J., and Stickle, George W.: Full-Scale Tests of N.A.C.A. Cowlings. NACA Rep. No. 592, 1937.

4. Nickle, Ferril R., and Freeman, Arthur B.: Full-Scale Wind-Tunnel Investigation of Wing Cooling Ducts. NACA ACR, Oct. 1938.

TABLE I

COMPARISON OF PRINCIPAL AERODYNAMIC CHARACTERISTICS OF THE MODEL WITH LIQUID-COOLED AND AIR-COOLED ENGINE INSTALLATIONS

Model arrangement	C_D (a) $C_L=0.25$	η_{max} $\beta=23\frac{1}{2}^\circ$	(b) η_t	$C_{L_{max}}$ $\delta_f=0^\circ$	$C_{L_{max}}$ $\delta_f=60^\circ$	$(L/D)_{max}$	V_{max} level flight
Model without nacelles, bare wing	0.0178	--	100	1.28	--	20.0	--
Air-cooled engine installation with large exit slot and oil coolers open	.0245	82.5	60	--	--	--	192
Air-cooled engine installation with large exit slot without oil coolers	.0238	82.5	62	1.34	1.73	15.8	194
Air-cooled engine installation with refaired exit slot with oil coolers closed	.0225	81.0	64	1.35	--	16.5	195.5
Air-cooled engine installation without cooling air with oil coolers closed	.0208	81.0	69	1.32	--	16.9	200.5
Liquid-cooled engine installation with oil and Prestone radiators	.0223	81.0	64.5	1.16	(c) 1.69	16.6	195
Liquid-cooled engine installation with oil radiators and without Prestone radiators	.0199	81.0	72.5	--	--	--	204
Liquid-cooled engine installation without oil and Prestone radiators	.0192	81.0	75	--	--	--	207

(a) From data at 100 m.p.h. test air speed.

(b) Based on $C_L = 0.25$ and η_{max} for $23\frac{1}{2}^\circ$.

(c) Landing gear extended; all others, landing gear retracted.

FIGURE LEGENDS

Figure 1.- Bare wing model.

Figure 2.- Model with nacelles for air-cooled engines.

Figure 3.- Model with nacelles, radiators, and oil coolers for liquid-cooled engines.

Figure 3a.- (Botton view) Model with nacelles, radiators, and oil coolers for liquid-cooled engines.

Figure 4.- Diagram of model arrangements.

Figure 5.- Blade dimensions for model propellers.

Figure 6.- Aerodynamic characteristics of model; without nacelles, radiators, or oil coolers. Approximate test air speed, 60 miles per hour.

Figure 7.- Aerodynamic characteristics of model; nacelles for air-cooled engines, large exit slots, oil coolers closed; approximate test air speed, 60 miles per hour.

Figure 8.- Aerodynamic characteristics of model. Nacelles for liquid-cooled engines, Prestone radiators on, oil coolers open; approximate test air speed, 60 miles per hour.

Figure 9.- Aerodynamic characteristics of model. Nacelles for air-cooled engines; oil radiators closed; exit slot refaired; approximate test air speed, 60 miles per hour.

Figure 10.- Aerodynamic characteristics of model. Nacelles for air-cooled engines; oil radiators closed; no cooling air; approximate test air speed, 60 miles per hour.

Figure 11.- Scale effect on drag coefficients for model arrangements with nacelles for air-cooled engines. $C_L = 0.25$.

Figure 12.- Scale effect on drag coefficient for model arrangements with nacelles for liquid-cooled engines. $C_L = 0.25$.

Figure 13.- Scale effect on increments of drag for the air-cooled and liquid-cooled engine-nacelle arrangements.

Figure 14.- Propulsive characteristics of the model with nacelles for air-cooled engines for four blade angles. Large cowling exit slots. $C_L = 0.25$.

Figure 15.- Propulsive characteristics of the model with nacelles for air-cooled engines at $\beta = 28\text{-}1/2^\circ$ for:

a. Model with cowling exit slot refaired; $C_L = 0.25$.
b. Model with no cooling air; $C_L = 0.25$.

Figure 16.- Propulsive characteristics of the model with nacelles for liquid-cooled engines for four blade angles; oil coolers open; Prestone radiators on; $C_L = 0.25$.

Figure 17.- Effect of power on lift coefficient for the model with nacelles for air-cooled engines. Large cowling exit slots; oil coolers closed; $\delta_f = 0^\circ$; approximate test air speed, 50 miles per hour.

Figure 18.- Effect of power on lift coefficient for the model with nacelles for air-cooled engines. Large cowling exit slots; oil coolers closed; $\delta_f = 60^\circ$; approximate test air speed, 50 miles per hour.

Figure 19.- Effect of power on the maximum lift coefficient and on the lift curve slope for the model with nacelles for air-cooled engines. Large cowling exit slots; oil coolers closed; approximate test air speed, 50 miles per hour.

Figure 20.- Effect of power on the pitching-moment coefficient for the model with nacelles for air-cooled engines. Large cowling exit slots; oil coolers closed; $\delta_f = 0^\circ$.

Figure 21.- Effect of power on the pitching-moment coefficient for the model with nacelles for liquid-cooled engines. Prestone radiators on; oil coolers open.

Figure 22.- Effect of power on the pitching-moment coefficient for the model with nacelles for air-cooled engines. Large cowling exit slots; oil coolers closed; $\delta_f = 60^\circ$.

Figure 23.- Speed determination for the model arrangements with nacelles for air-cooled engines. Based on constant-speed propeller operation with: total engine power, 4,000 horsepower; propeller speed, 1,300 r.p.m.; propeller diameter, 13 feet; gross weight, 70,570 pounds; wing area, 2,750 square feet.

Figure 24.- Speed determination for the model arrangements with nacelles for liquid-cooled engines. Based on constant-speed propeller operation with: total engine power, 4,000; propeller speed, 1,300 r.p.m.; propeller diameter, 13 feet; gross weight, 70,570 pounds; wing area, 2,750 square feet.

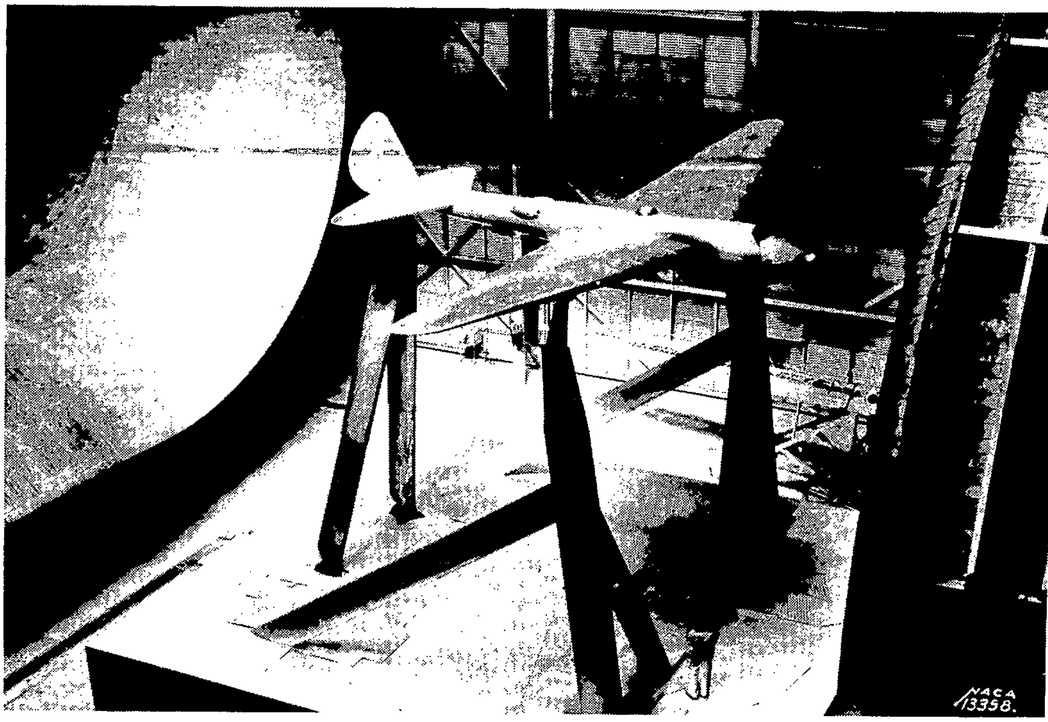

Figure 1

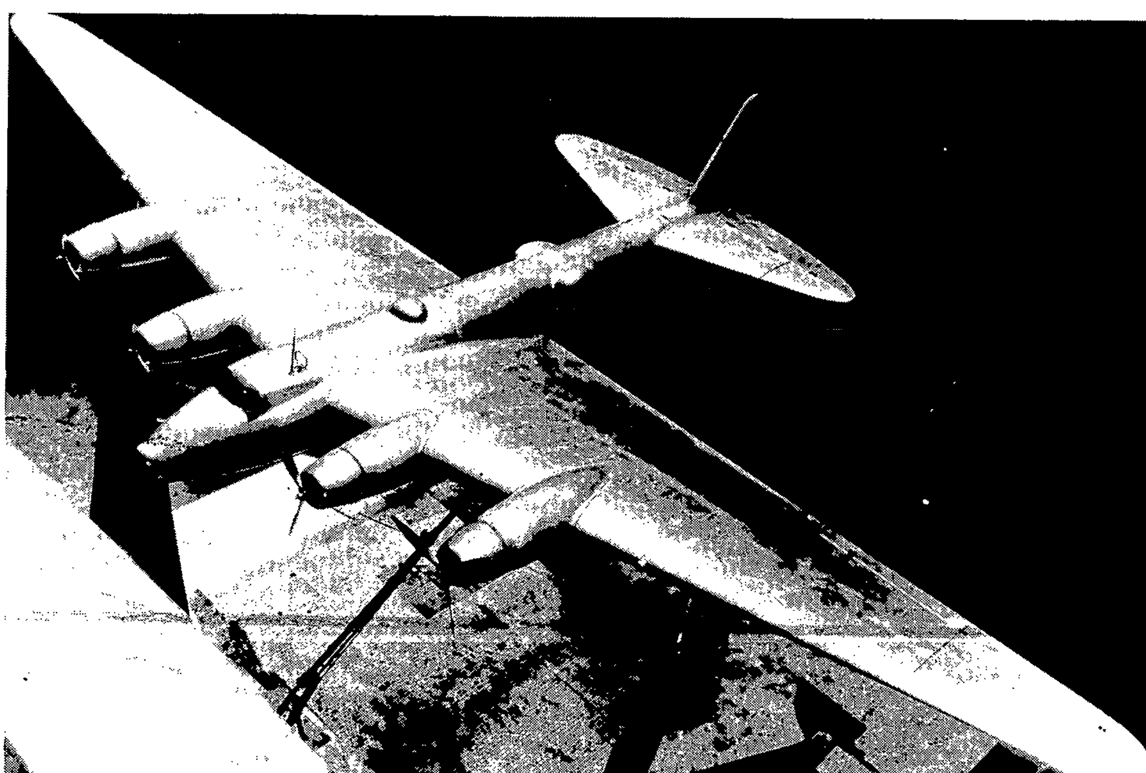

Figure 2

Figure 3

Figure 3a

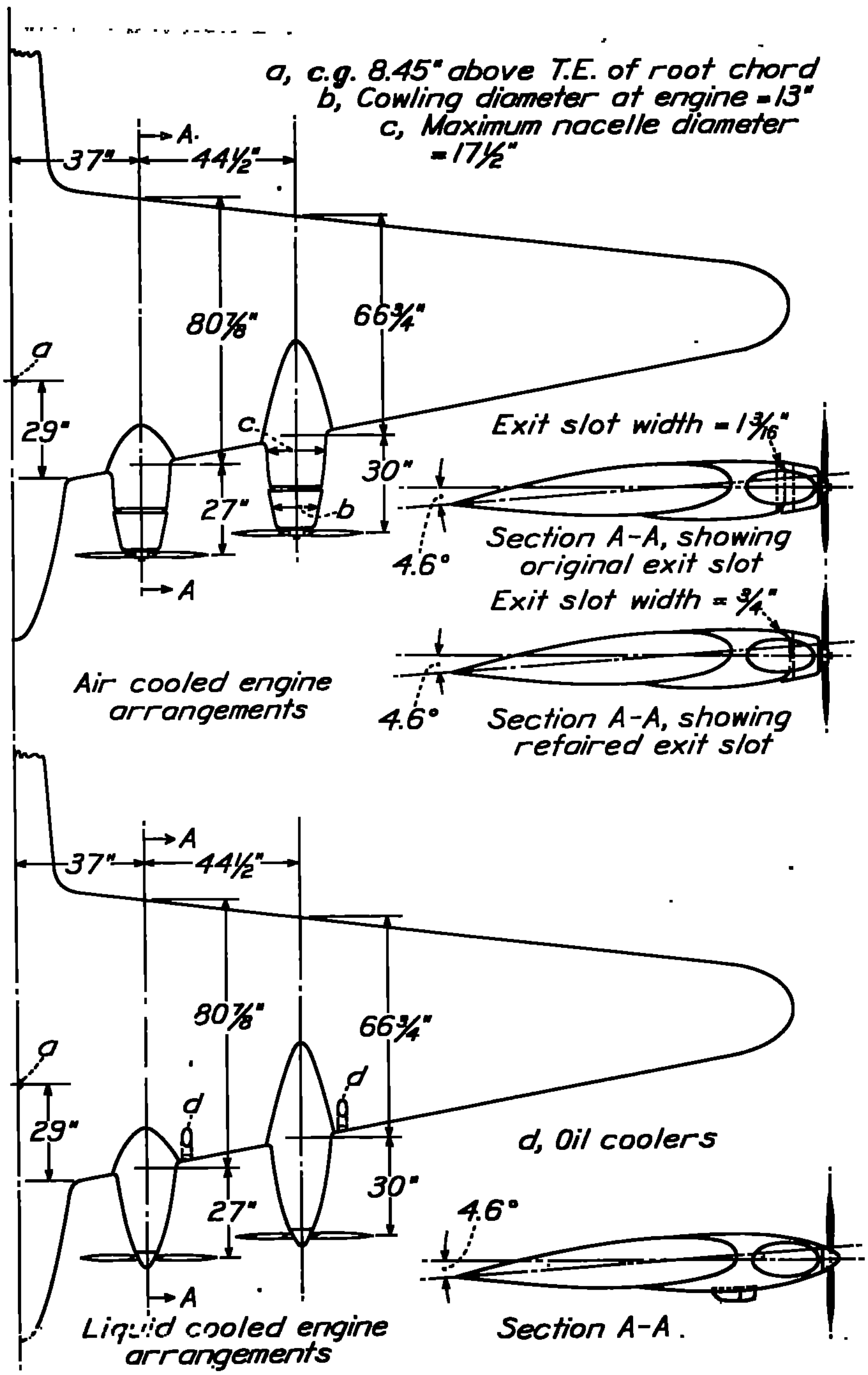
a, c.g. 8.45" above T.E. of root chord
b, Cowling diameter at engine = 13"
c, Maximum nacelle diameter = 17½"
37"
44½"
A
80⅞"
66¾"
a
29"
c
27"
b
30"
Exit slot width = 1 3/16"
Section A-A, showing original exit slot
4.6°
Exit slot width = ¾"
Air cooled engine arrangements
Section A-A, showing refaired exit slot
d
d, Oil coolers
Section A-A.
Liquid cooled engine arrangements

Figure 4

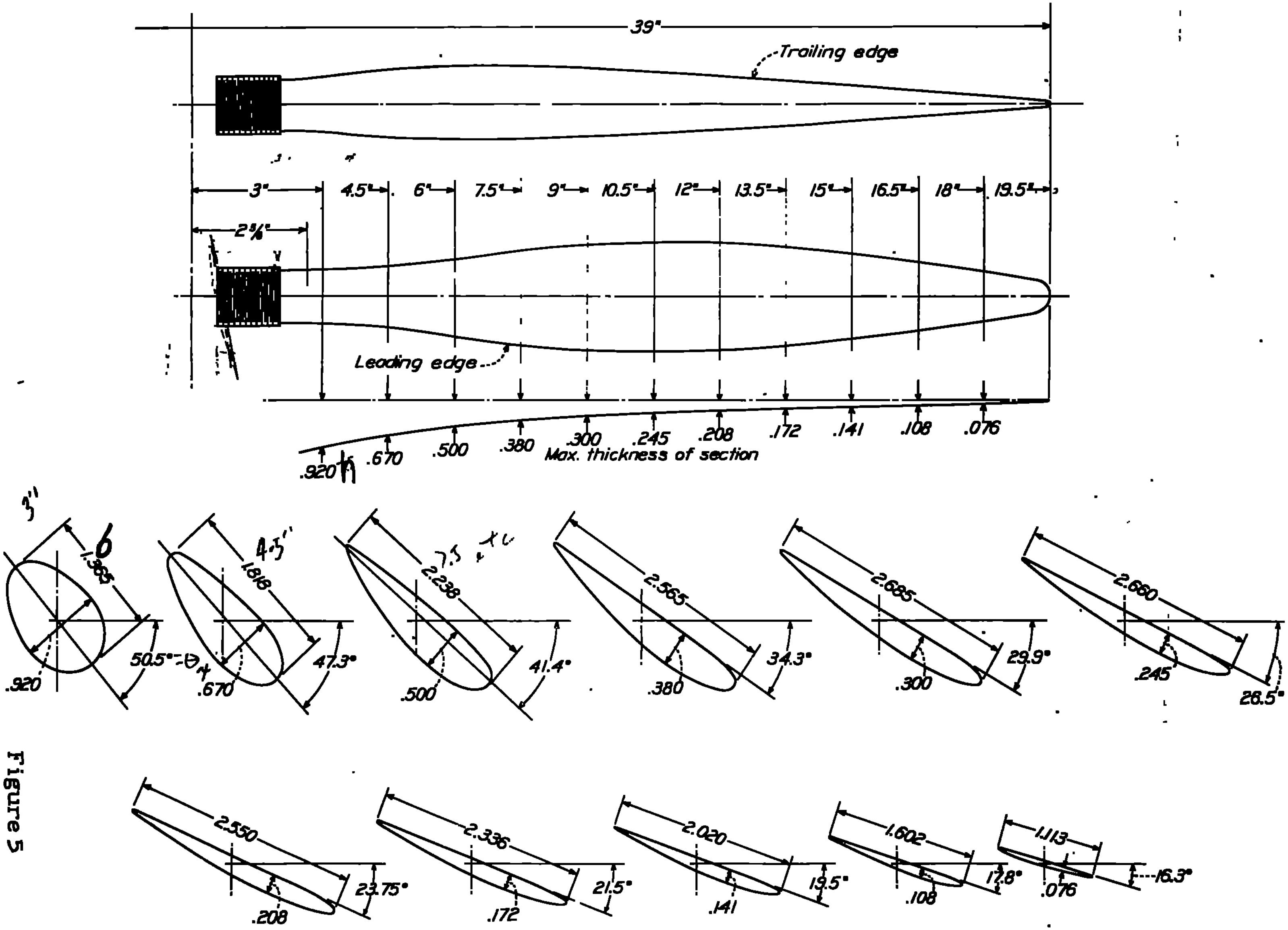
39"
Trailing edge
3"
4.5"
6"
7.5"
9"
10.5"
12"
13.5"
15"
16.5"
18"
19.5"
2⅝"
Leading edge
.920
.670
.500
.380
.300
.245
.208
.172
.141
.108
.076
Max. thickness of section
1.385
50.5°
1.818
47.3°
2.238
41.4°
2.565
34.3°
2.685
29.9°
2.660
26.5°
2.550
23.75°
2.336
21.5°
2.020
19.5°
1.602
17.8°
1.113
16.3°

Figure 5

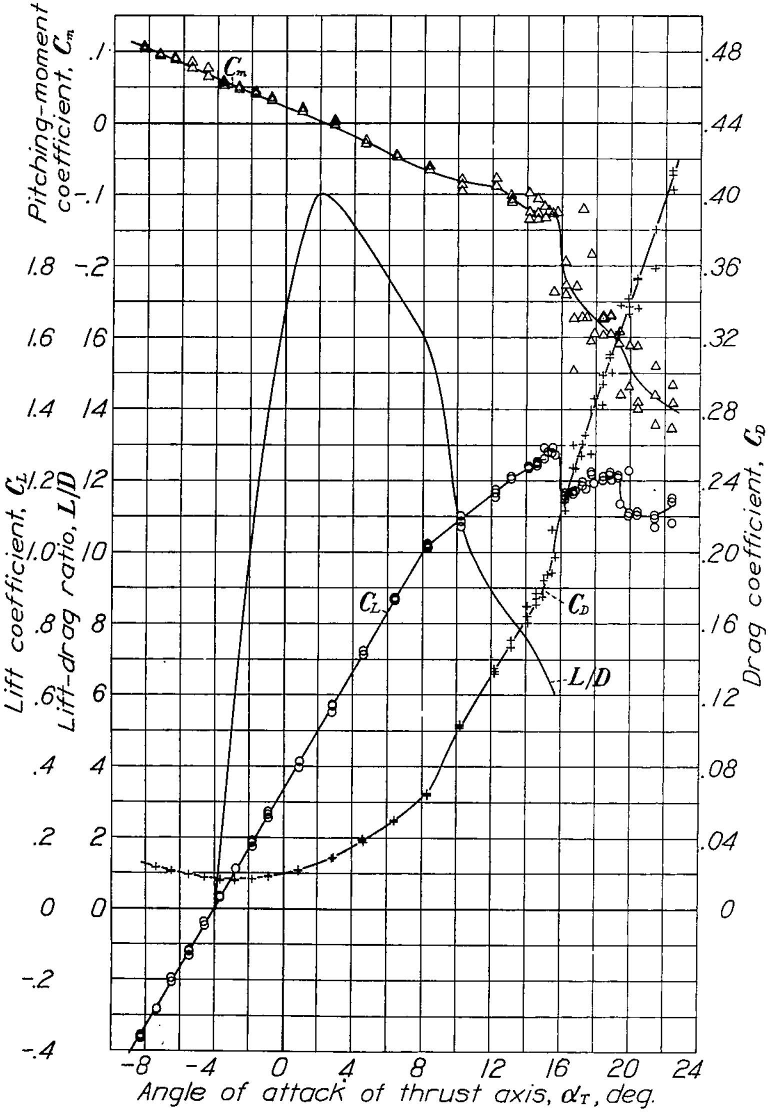

Figure 6

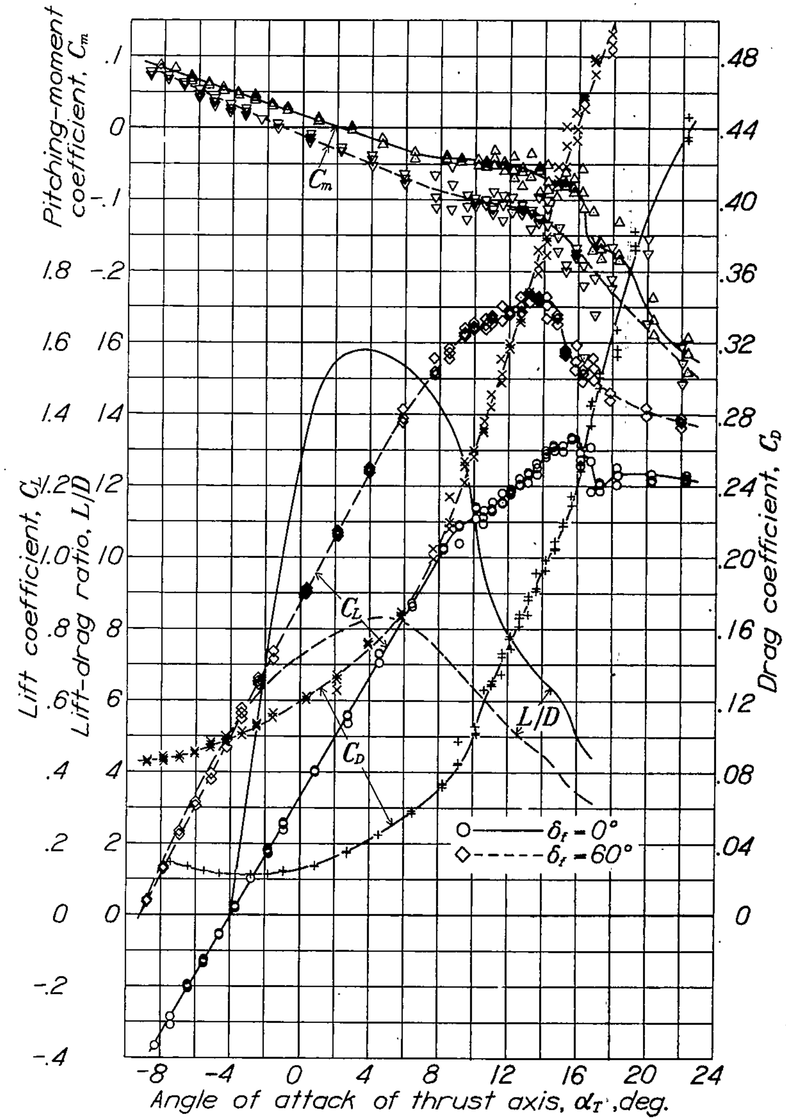

Figure 7

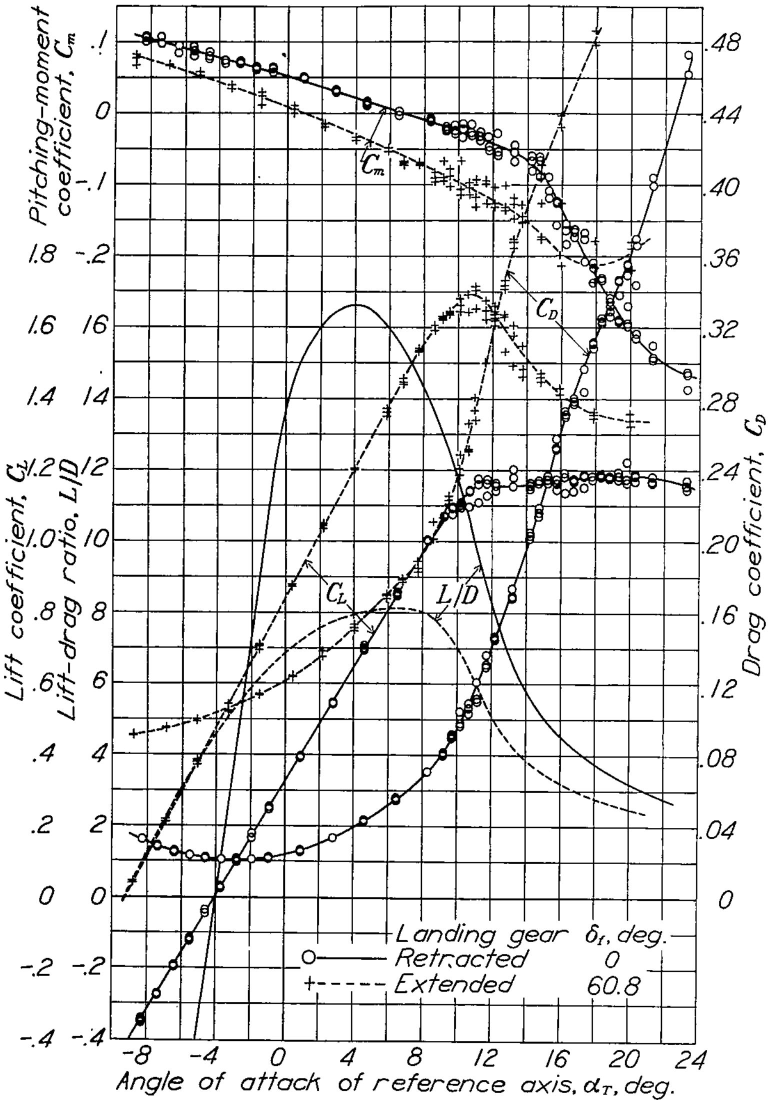

Figure 8

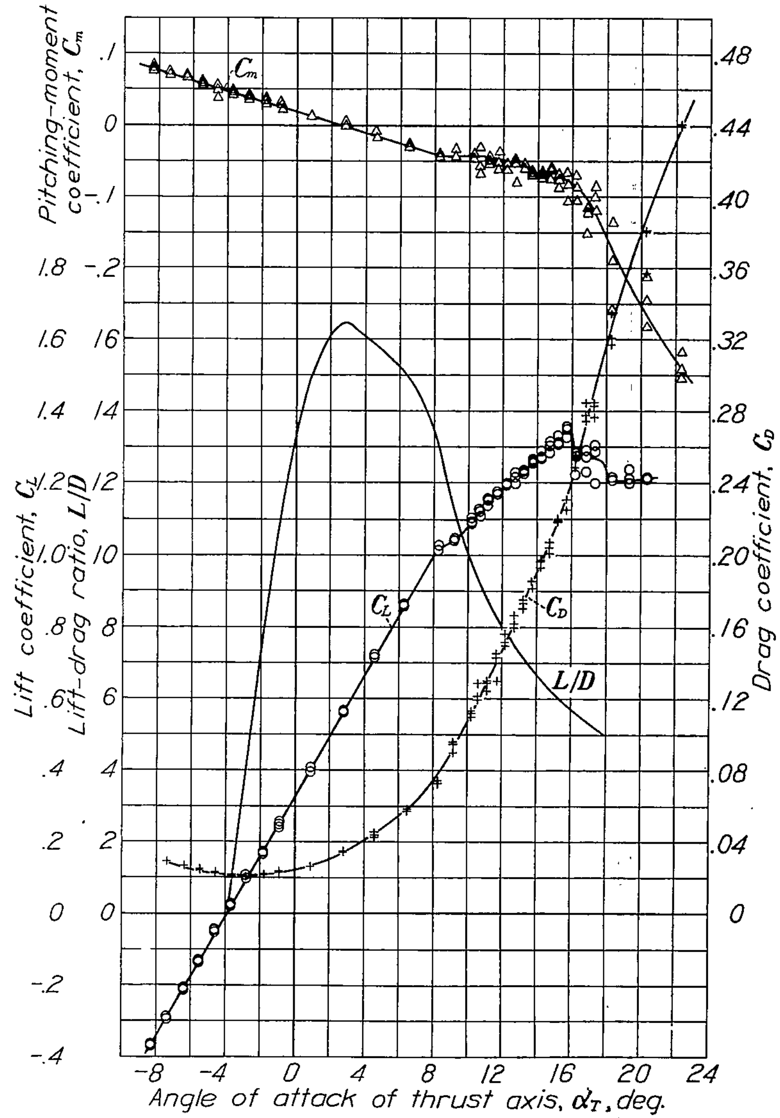

Figure 9

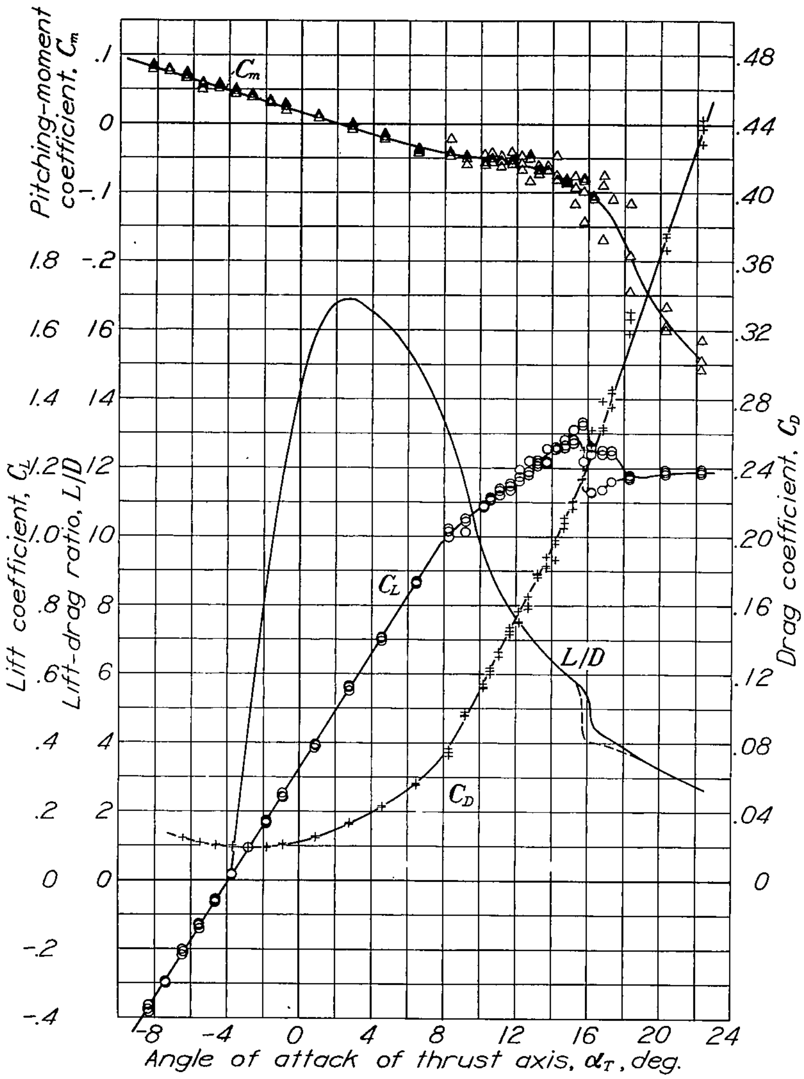
Pitching-moment coefficient, C_m
Lift coefficient, C_L
Lift-drag ratio, L/D
Drag coefficient, C_D
C_m
C_L
C_D
L/D
Angle of attack of thrust axis, α_T, deg.

Figure 10.

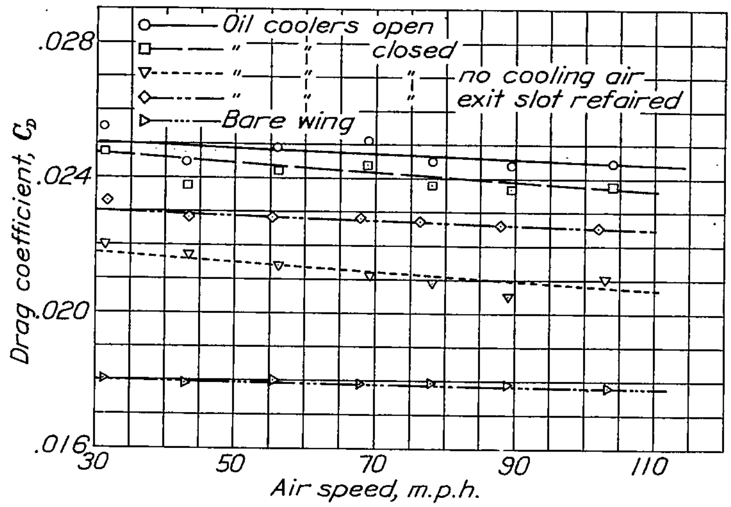

Figure 11

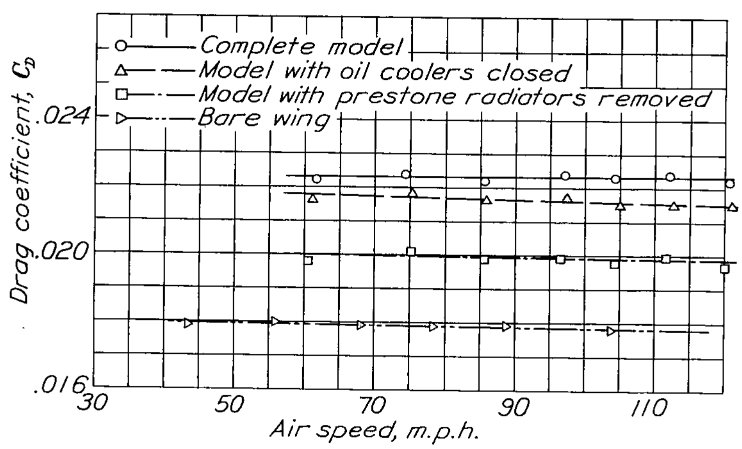

Figure 12

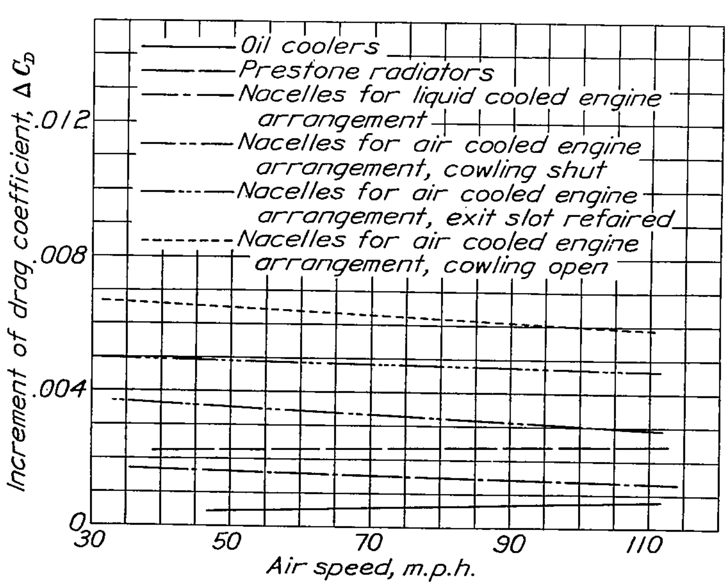

Figure 13

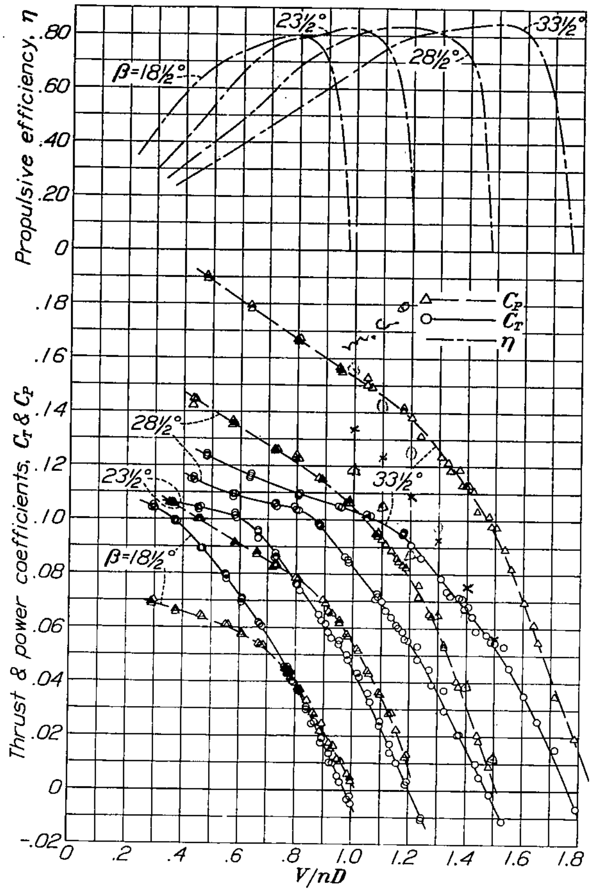

Figure 14

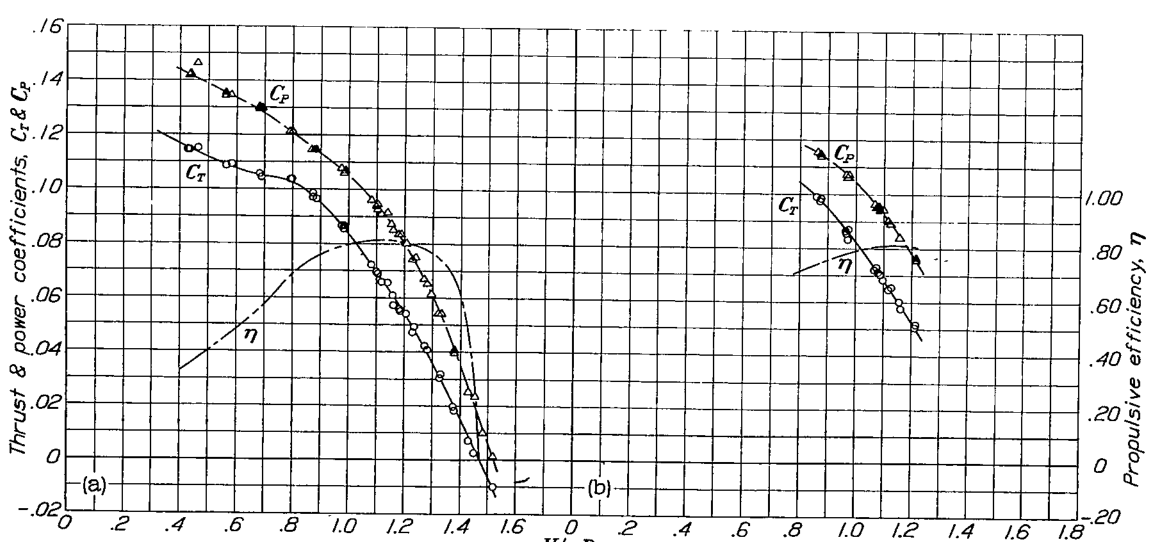

Figure 15

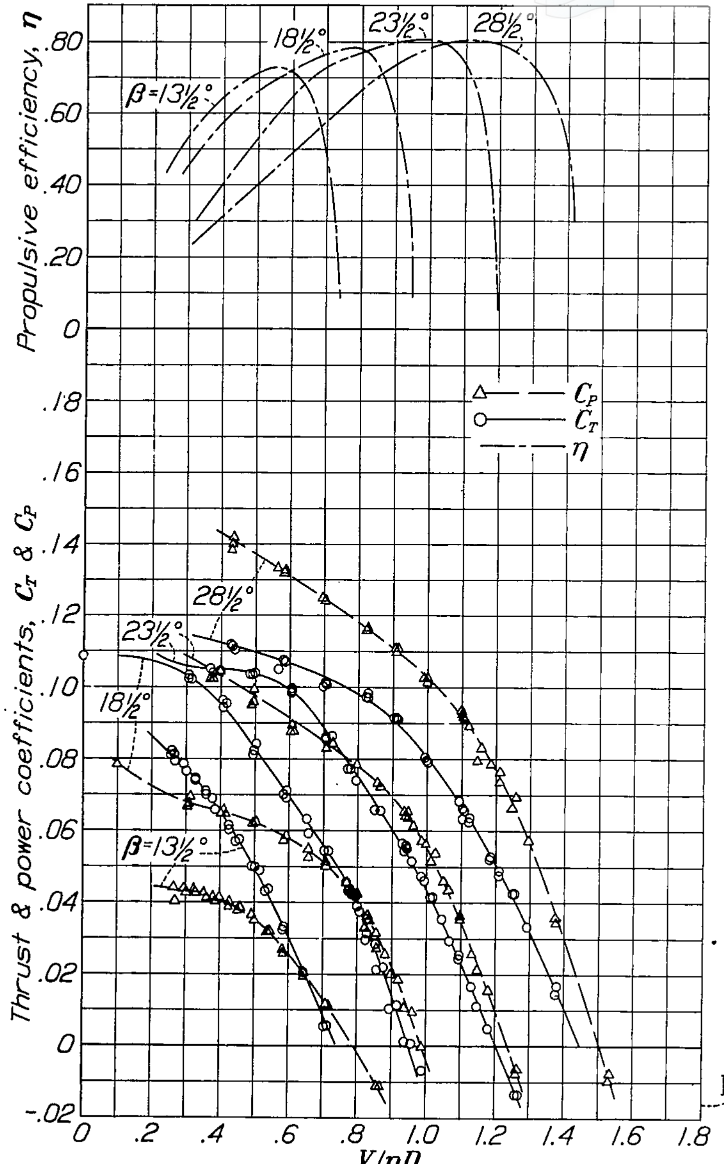

Figure 16.

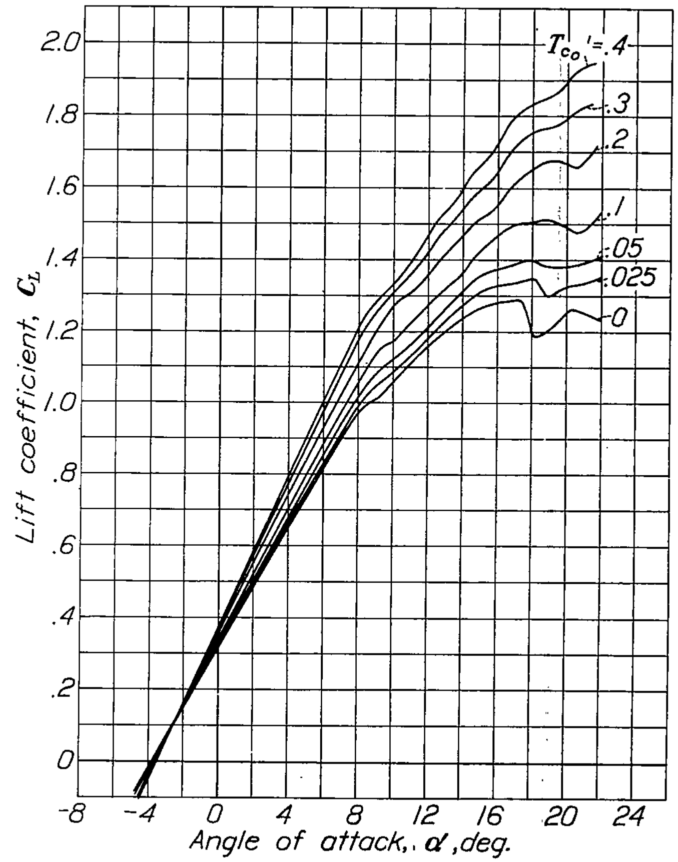

Figure 17.

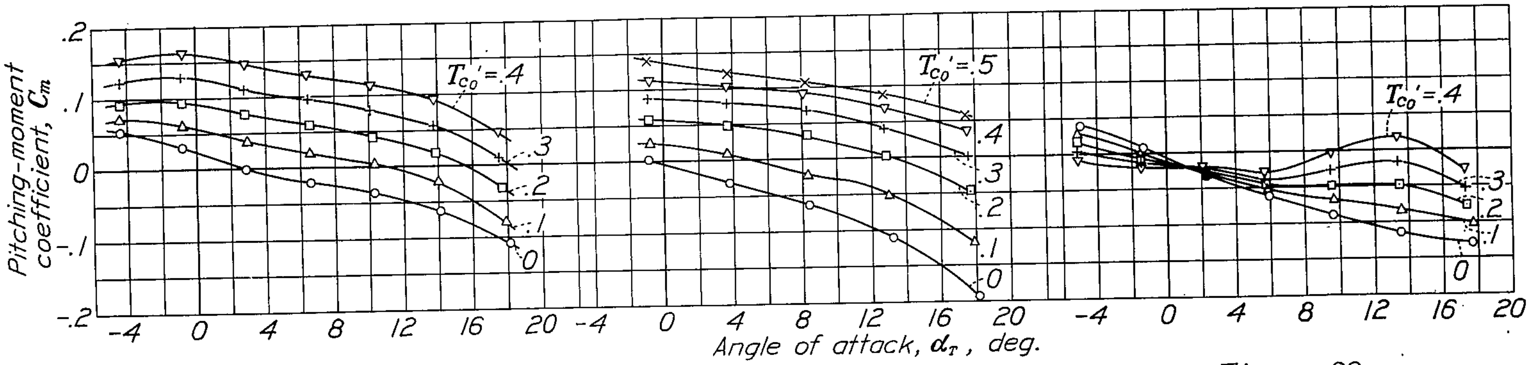

Figure 20

Figure 21

Figure 22

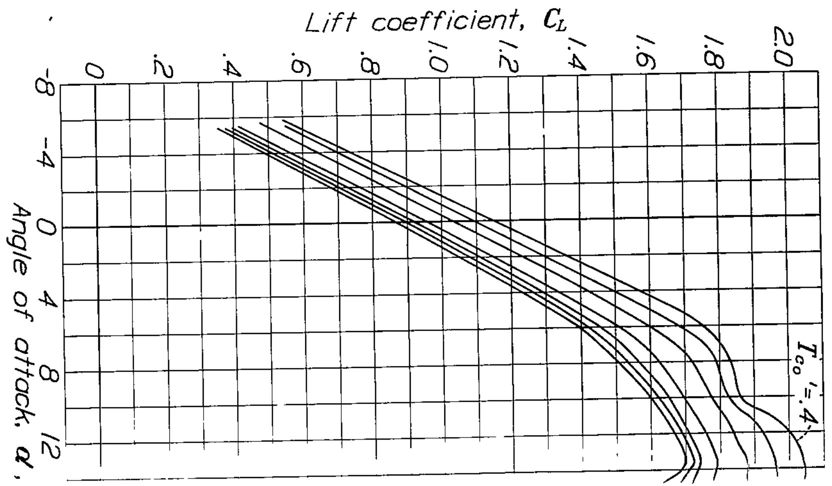

Figure 18

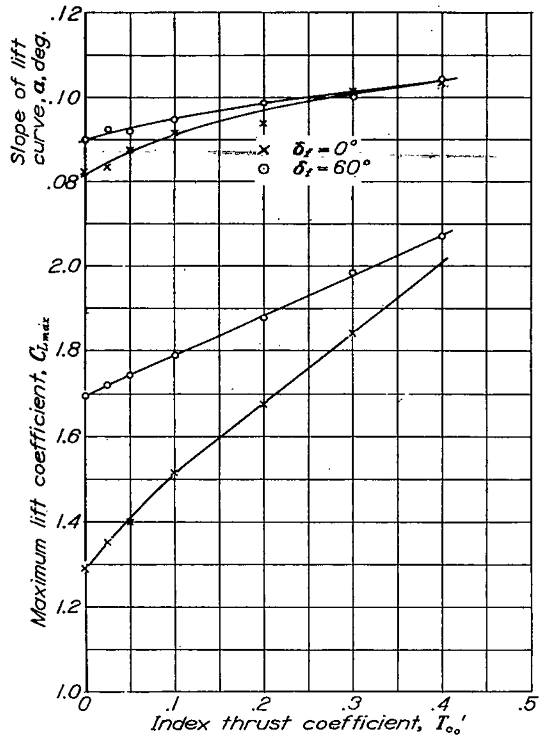

Figure 19

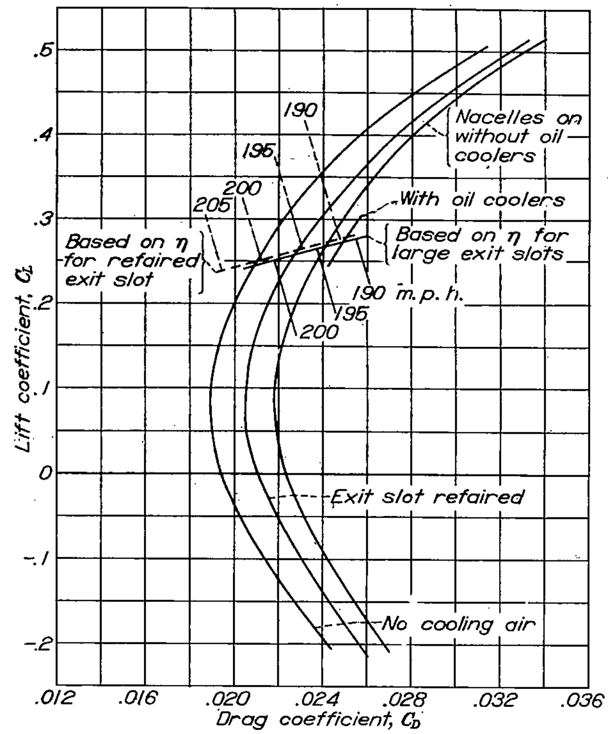

Figure 23

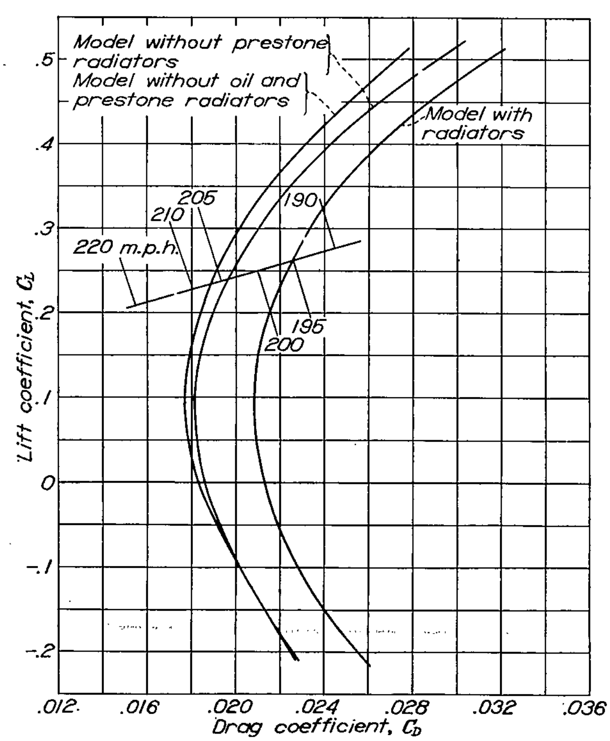

Figure 24